

XMM-Newton observations of EF Eridani: the textbook example of low-accretion rate polars[★]

A.D. Schwone¹, A. Staude¹, D. Koester², and J. Vogel¹

¹ Astrophysikalisches Institut Potsdam, An der Sternwarte 16, D-14482 Potsdam
e-mail: aschwope@aip.de

² Institut für Theoretische Physik und Astrophysik, Universität Kiel, 24098 Kiel, Germany

Received ; accepted

ABSTRACT

Archival X-ray observations of EF Eridani obtained in a low state revealed distinct X-ray detections at a luminosity $L_X \simeq 2 \times 10^{29} \text{ ergs}^{-1}$, three orders of magnitude below its high state value. The plasma temperature was found to be as low as $kT \lesssim 2 \text{ keV}$, a factor 10 below the high state. The X-ray/UV/IR spectral energy distribution suggests faint residual accretion rather than coronal emission as being responsible for the low-state X-ray emission. EF Eri thus showed a clear transition from being shock-dominated in the high state to be cyclotron-dominated in the low state. From the optical/UV spectral energy distribution we re-determine the photospheric temperature of the white dwarf to $\sim 10000 \text{ K}$. Contrary to earlier claims, WD model atmospheres produce sufficient UV flux to reproduce the published *GALEX* flux and orbital modulation.

Key words. stars: individual: EF Eri – stars: X-ray – stars: cataclysmic variables

1. Introduction

Polars are magnetic cataclysmic binaries consisting of a late-type main-sequence star and a strongly magnetic white dwarf locked in synchronous rotation. EF Eri was one of the 11 polars known in the pre-ROSAT era, it was the second brightest at optical and at X-ray wavelengths after the prototypical system AM Herculis. It was studied with all major X-ray observatories (EINSTEIN, EXOSAT, GINGA, ROSAT) in the past and was always found in a high accretion state.

EINSTEIN observations revealed the presence of uncorrelated soft and hard X-ray emission and were used to observationally establish the standard picture of magnetic accretion onto white dwarfs in the high \dot{m} -regime dominated by a shock-heated accretion column and cooling by free-free radiation (Beuermann, Stella & Patterson 1987, henceforth BSP87). The absence of a pronounced soft X-ray excess made BSP87 to coin EF Eri the textbook example of AM Herculis-type systems. The shape of the X-ray light curves, in particular the presence of a soft X-ray absorption dip, was used to uncover the accretion geometry. EF Eri had a main accretion pole which was continuously in view, the observer has a moderate inclination with respect to the orbital plane, so that the line of sight crosses the accretion stream on its way through the magneto-

sphere. This special geometry allowed detailed stream-density diagnostics with GINGA and EXOSAT (Watson et al. 1989).

The accretion geometry was intensively studied using photo- and spectro-polarimetric data (e.g. Bailey et al. 1982, Cropper 1985, Pirola et al. 1987, Meggitt & Wickramasinghe 1989, Beuermann et al. 2007). The latter three papers agree that the white dwarf's magnetic field is probably more complex than that of a centered dipole. The zero point of Bailey's ephemeris (Bailey et al. 1982) centered on the IR (X-ray) absorption dip is widely used in the literature. Pirola et al. (1987) determined an updated orbital period based on a linear regression of the arrival times of linear polarisation pulses. Beuermann et al. (2007) derived a slightly revised ephemeris by including the ROSAT PSPC X-ray dip timings from July 1990. Phases in this paper refer to Bailey's phase zero and Pirola's period.

EF Eri turned into a deep low state at $V \simeq 18$ in 1997 (Wheatley & Ramsay 1998) and remains therein since then. A re-brightening was reported in VSNET on March 5, 2006 (ERI EF 20060305.724 at 14.2 unfiltered CCD based on the Henden-Sumner sequence), but the system returned to the low state shortly thereafter. While in the high state the stellar photospheres are outshone by accretion radiation, the low state offers the opportunity to investigate the stars, at least in principle. Since EF Eri is the polar with the shortest orbital period, $P_{\text{orb}} = 81 \text{ min}$, just a few minutes above the CV minimum period, low state observations are of utmost importance to test current scenarios of CV evolution and to search for the cool

[★] Based on observations obtained with XMM-Newton, an ESA science mission with instruments and contributions directly funded by ESA Member States and NASA

Table 1. XMM-Newton observations of EF Eri. The first column lists the unique observation ID and the revolution number of the spacecraft, the last column lists the nominal and effective exposures times of the individual observations, the latter quantity after screening for high background and other instrumental defects.

OBSID/rev	Date	Instr.	Exp Nom/Eff (s)
0111320201/496	2002-08-24	EPIC-PN	6132/1859
		OM V	6000
0111320401/571	2003-01-20	EPIC-MOS	5160/5088
0111320501/583	2003-02-14	EPIC-PN	5047/4559
		EPIC-MOS	6660/6575
		OM V	3400
		OM UVW1	2600

secondary. Indeed, following the more indirect conclusion by Beuermann et al. (2000) of a substellar secondary in EF Eri from the non-detection of any spectral signature of the companion in optical spectra, Howell & Ciardi (2001) claimed the detection of the secondary in near-infrared spectra. A more likely explanation of the observed infrared humps was given in terms of cyclotron radiation (Beuermann et al. 2000, Harrison et al. 2004).

Beuermann et al. (2000) also estimated the photospheric temperature of the white dwarf from their low-resolution optical spectra, $T_{\text{WD}} = 9500 \pm 500$ K, one of the coldest WDs among all CVs. This allowed to draw some conclusions on the likely evolutionary state of the object. Recently, Szkody et al. (2006) report on phase-resolved *GALEX* observations with the puzzling result of a distinct source of ultraviolet flux much larger than the underlying 9500 K white dwarf.

Here we report on archival XMM-Newton observations of EF Eri obtained in a low accretion state. We search for remaining X-ray emission in the low state either originating from the white dwarf or the secondary and analyse the data from the optical monitor taken through two different filters.

2. Low-state observations with XMM-Newton

The XMM-Newton Science Archive (XSA) contains three observations of the X-ray sky in the direction of EF Eri. They are listed with their nominal exposure times in Tab. 1.

We refer to individual observations by an 'E' followed by the last three digits of the OBSID, i.e. E201 for the observation on 28th of April, 2002. All X-ray observations were obtained in full frame mode. The RGS did not reveal useful data due to low count rate and will not be considered further. Data processing was performed with the latest version of the XMM-Newton SAS (version 7.0), a spectral analysis of the X-ray data was performed with XSPEC. Despite the relatively short exposure times, almost full phase coverage of the $P_{\text{orb}} = 81$ min binary was achieved at two occasions (E401 and E501). The accumulated phase uncertainty of the period derived by Piirola et al. (1987) at the epoch of the last XMM-Newton X-ray observation, i.e. after ~ 155000 binary cycles, is 0.014 phase units only and thus negligible.

EPIC-MOS and EPIC-PN show a faint apparent companion to EF Eri at $\alpha(2000) = 03^h14^m14.0$ and $\delta(2000) = -22^\circ36'04''$. The source has no counterpart on DSS2 images. It contributes at a level of $F_X \simeq 1.5 \times 10^{-14}$ erg cm $^{-2}$ s $^{-1}$ in the 0.1 – 10 keV band. This source could not be resolved in all previous X-ray observations with other satellites. Its faint flux was just a small contamination of all previous X-ray observations and thus irrelevant. It represents, however, a $\sim 20\%$ contamination of the flux of EF Eri during XMM-Newton observations. We thus chose source and background regions for the extraction of light curves and spectra avoiding the region around this source.

2.1. X-ray spectra and light curves

The net exposure time of observation E201 was just 1859 s. The source was detected with EPIC-PN at a mean count rate of 0.022 s $^{-1}$. The spectrum contains no photons above 5 keV, it could be successfully fitted (reduced $\chi^2 = 0.93$ for 9 degrees of freedom) with a cooling plasma model (MEKAL in XSPEC terms) with a temperature of $kT = 2.8 \pm 1.7$ keV only very little affected by interstellar absorption. In general, all X-ray spectral fits based on XMM-Newton observations are compatible with zero interstellar absorption, in accord with the low column density inferred from ROSAT and EXOSAT, $N_{\text{H}} = 10^{19}$ cm 2 (Beuermann et al. 1991; Watson, King & Williams 1987), and from EINSTEIN, $N_{\text{H}} < 1 \times 10^{20}$ cm 2 (BSP87). The integrated flux in this component was $F_X = 7 \times 10^{-14}$ erg cm $^{-2}$ s $^{-1}$ (0.1 – 10 keV).

Observation E401 was performed with EPIC-MOS only and resulted in the detection of 26/20 photons in 5099/5088 s with MOS1/2, respectively. The spectrum was found to be very soft again, an unconstrained fit yielded $kT = 0.5 \pm 1$ keV, but the spectral parameters remained highly uncertain due to the small number of photons. A fit using the same parameters as for E501, see below, yielded a flux of $F_X \simeq 4 \times 10^{-14}$ erg cm $^{-2}$ s $^{-1}$ (0.1 – 10 keV), slightly indicative of a lower X-ray flux at that epoch.

Observation E501 was performed with all three X-ray cameras onboard and revealed 140, 43, and 40 source photons with EPIC-PN, MOS1, and MOS2, respectively. The mean spectrum, which is a good approximation to the orbital mean spectrum also, is shown in Fig. 1. Again, it is a soft spectrum which could be fitted with just one emission component (reduced $\chi^2 = 0.81$ for 33 d.o.f.). The best-fit plasma temperature of the MEKAL model is $kT = 1.7 \pm 0.2$ keV, and the integrated flux $F_X = 6 \times 10^{-14}$ erg cm $^{-2}$ s $^{-1}$ (0.1 – 10 keV). The $O - C$ residuals of such a fit (see Fig. 1) give the slight impression of a systematic trend with an excess of photons between 0.5–1.0 keV. However, the parameters of any additional spectral component cannot be constrained significantly and we thus stick to a one component X-ray spectrum.

We found no significant X-ray variability of the total X-ray flux between the three XMM-Newton observations. X-ray variability in E501, the longest of the three observations, was almost insignificant. A binned light curve with bin size 243 s (20 phase bins per orbital cycle) shows one bin with no source photon. It occurs at phase 0.7, i.e. it cannot be associated with

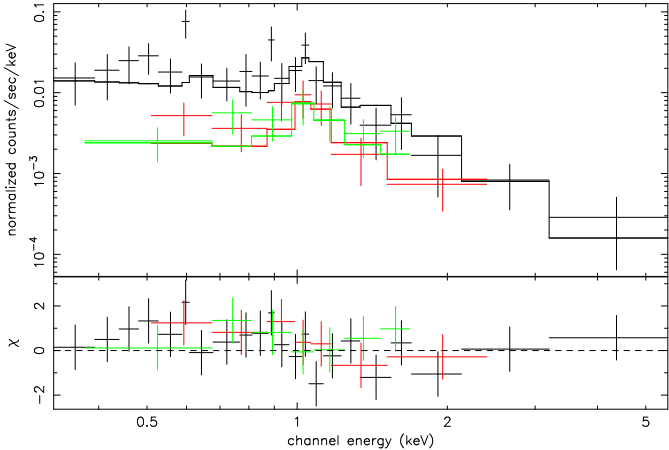


Fig. 1. Mean X-ray spectrum of EF Eri (observation E501) and best-fit thermal plasma model.

the high state absorption dip (if the accuracy of Piirona's period is as high as the formal uncertainties given in their suggest). Given the small number of X-ray photons a secure claim on the existence of a dip cannot be made.

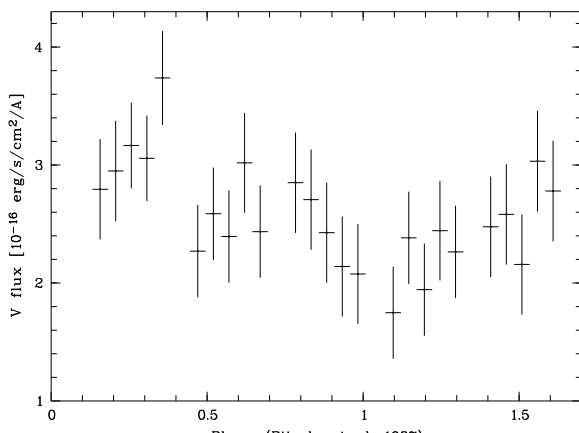


Fig. 2. OM light curve through V-filter from observation E201. The bin size is 243 s corresponding to 0.05 phase units.

2.2. Optical/UV observations with the OM

The optical monitor OM was used in observations E201 and E501 with the V and UVW1 filters, respectively (see Tab. 1 for details). In E201 full phase coverage was achieved, in E501 only parts of the orbital cycle were covered with the two filters. During E201, the mean countrate in the V-filter (phase 0.16 – 1.61) was $0.88(8)\text{s}^{-1}$ corresponding to a mean flux of $F_V = 2.6(2) \times 10^{-16} \text{ erg cm}^{-2} \text{ s}^{-1} \text{ Å}^{-1}$. During E501 the mean countrate through the V-filter (phase interval 0.90 – 1.55) was $0.87(5)\text{s}^{-1}$ corresponding to $F_V = 2.2(1) \times 10^{-16} \text{ erg cm}^{-2} \text{ s}^{-1} \text{ Å}^{-1}$, and through the UVW1-filter (phase interval 0.67 – 1.17) it was $1.32(4)\text{s}^{-1}$ corresponding to $F_{UVW1} = 6.5(2) \times 10^{-16} \text{ erg cm}^{-2} \text{ s}^{-1} \text{ Å}^{-1}$.

Some modulation of the optical flux at a level of about 50% was discovered in E201 (Fig. 2) with a minimum around phase zero. The low-state light curves by Skody et al. (2006) show a minimum at phase 0.4. The phase difference between the two epochs by using either Bailey's period used by Skody et al. (2006) and Piirona's period used here is negligible, 0.01 phase units. Hence, this phase shift, if a real feature of the light curve, cannot be explained by different phase conventions. However, both data sets were obtained with small telescopes and are rather noisy. Given the rather large error bars on individual light curve bins we are not further discussing possible differences between the light curves. We note, however, that the accumulated phase difference from Bailey's zero point in 1979 to the epochs of the GALEX (2004) or XMM-Newton (2003) observations is 0.18 phase units with either Bailey's or Piirona's period and thus not negligible. Formally, the period derived by Piirona et al. should be preferred due to the claimed higher accuracy, but an independent re-determination of the linear polarization ephemeris is highly desirable, should EF Eri ever return to a high accretion state.

The UVW1-filter is centered on 2910Å, between the GALEX-NUV passband (Skody et al. 2006) and the optical broad-band filters. Mean flux values as measured with the OM are shown together with other low-state photometric and spectroscopic data (Harrison et al. 2004, Skody et al. 2006) from the infrared to the ultraviolet spectral range in Fig. 3. It shows that the different low state observations are compatible with each other.

Based on an analysis of their low-state GALEX ultraviolet and optical photometry Skody et al. (2006) state the existence of a light-source reminiscent of a 20000 K hot spot. Their spot model, however, could neither explain the large-amplitude FUV variations nor the spectral energy distribution and they arrive at the conclusion, that *no* spot model can explain their observations.

The analysis by Skody et al. (2006) was based on an assumed effective temperature $T_{\text{eff}} = 9500\text{ K}$ (Beuermann et al. 2000) which they approximated as a Planckian function. We note, that this approximation indeed gives rise to a large ultraviolet excess. We re-address the question of the white dwarf and spot temperature making use of state-of-the-art white dwarf model atmospheres (Koester et al. 2005 and references therein). The optical spectrum alone is best described by a model with $T_{\text{eff}} = 10500 \pm 1000\text{ K}$. This value is in accord with the more recent analysis by the Göttingen group (Beuermann et al. 2007) who used $T_{\text{eff}} = 11000 \pm 1500\text{ K}$.

The pure white dwarf model falls short of matching the observed ultraviolet flux. We therefore fitted the SED at orbital minimum and maximum and the ultraviolet/optical light curves with a two-temperature model, a cooler one representing the white dwarf and a hotter one representing a spot. We folded our white-dwarf model spectra with the effective area curves of the two GALEX passbands¹ thus converting Eddington flux to count rate. Size, temperature and location of the spot and the temperature of the white dwarf were varied until a satisfactory fit (by eye) to the optical and ultraviolet light curves

¹ http://galexgi.gsfc.nasa.gov/tools/Resolution_Response/index.html

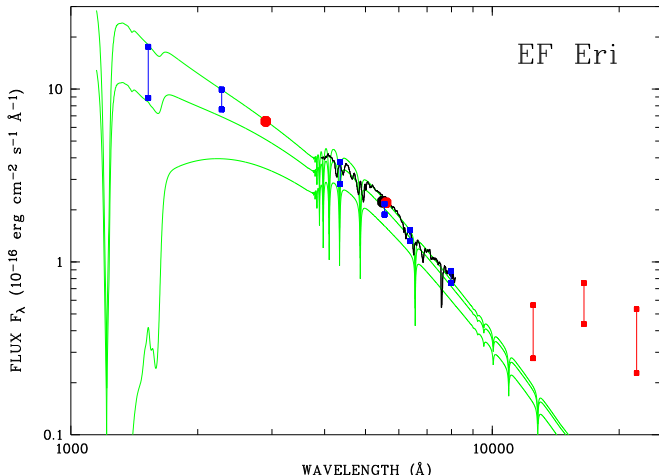


Fig. 3. Ultraviolet to infrared spectral energy distribution of EF Eri in the low state. Shown are an optical low-state spectrum and infrared JHK photometry adapted from Harrison et al. (2004), GALEX-UV and optical BVRI photometry from Szkody et al. (2006, blue dots), OM V-band and UVW1-photometry (red dots), and the result of our spectral synthesis with a two-temperature model (see text for details). Whenever possible, orbital minimum and maximum brightness are indicated and connected by lines

and the SED were reached. We arrived at a consistent solution for $T_{\text{wd}} = 9750$ K and $T_{\text{spot}} = 18500$ K with an estimated uncertainty of 1000 K in the white dwarf temperature. The spot temperature is subject to much larger systematic uncertainties, since e.g. our assumption of a uniform spot temperature is a very crude approximation. The model spectra shown in Fig. 3 at orbital minimum and maximum were computed for a binary inclination $i = 60^\circ$, a spot extent of 24° (half opening angle), and a spot colatitude of just 12.5° . A rather high inclination and a high 'northern' spot latitude, the spot undergoes a partial self-eclipse only, are required from the fact that the FUV-band is almost completely dominated by the spot. Even at orbital minimum the white dwarf contributes only $\sim 10\%$ to the total flux in that band (see the lowest model curve in Fig. 3). Our model is simple and far from being unique but it fits the data well and contradicts the conclusion by Szkody et al. (2006) that no spot model can explain both the SED and the variability.

Combining parallaxes, proper motions and absolute magnitude constraints, Thorstensen (2003) derived distance estimates for 14 CVs with a Bayesian method, among them EF Eri. Dependent on the proper-motion, magnitude and velocity priors, he derived a short, $d = 113^{+19}_{-16}$ pc, and a long, $d = 163^{+66}_{-50}$ pc, distance to EF Eri. At 113 pc the observed flux of our 9750 K white dwarf model results in a radius of 6.5×10^8 cm and implies a relatively massive white dwarf of $0.87 M_\odot$. At 163 pc the implied mass is $\sim 0.55 M_\odot$. These numbers differ slightly from those derived in Beuermann et al. (2000), since the spot contribution was taken into account in our analysis.

3. Results and discussion

We have analysed archival XMM-Newton observations of EF Eri obtained in 2002 and 2003. At all three occasions the polar was detected as an X-ray source, although at a very low flux level. The spectra were compatible with emission from a low-temperature corona-like plasma. The longest X-ray observation had almost full phase coverage, the plasma temperature was as low as 2 keV or less. The mean orbital integrated flux in this component is about $F_X = 6 \times 10^{-14}$ erg cm $^{-2}$ s $^{-1}$. Assuming isotropic radiation and a distance of 163 pc (Thorstensen 2003), a luminosity of $L_X \sim 2 \times 10^{29}$ erg s $^{-1}$ is derived.

The question arises if this faint X-ray flux originates from the corona of the secondary or from the accretion region on the white dwarf. Neither X-ray variability nor the X-ray spectrum give a clear answer. Both, a coronal plasma and the cooling plasma from low level accretion have such low temperatures as measured here. Evidence for X-ray emission from an accretion plasma can be given indirectly. Firstly, although not very much is known about X-ray emission from degenerate stars at the bottom of the main sequence, their X-ray luminosities seem to fall short by one dex with respect to the X-ray luminosity of EF Eri (Stelzer et al. 2006). Secondly, EF Eri shows clear signs of residual accretion via the detection of infrared cyclotron harmonics (Harrison et al. 2004). It therefore appears reasonable to assign the observed X-ray emission to some remaining weak accretion. This will be our working hypothesis in the following. It remains unclear if residual accretion happens via an accretion stream or via a stellar wind, the latter being inferred in order to explain the faint X-ray emission from the small group of pre-CVs (termed also LARPs, Schwone et al. 2002, Schmidt et al. 2005, Vogel et al. 2006). Since the emission region in EF Eri is not self-eclipsing (Beuermann et al. 1987, 1991), we are lacking a distinct photometric feature to discern between the two possibilities. The pronounced soft X-ray absorption dip as a sign of stream accretion and seen in high accretion states was not secularly detected here, but due to the small number of photons its absence does not give a clear-cut answer to the question of the accretion mode.

We discuss the energy balance of the accretion process in the low state on the assumption that the observed X-ray emission is due to accretion onto the white dwarf primary. We make the further assumption that the excess emission in the infrared over the extrapolated white dwarf spectrum is solely due to cyclotron emission from the accretion plasma. The relevant radiation components are shown in Fig. 4. It shows the coronal plasma in the X-ray regime and the cyclotron component in the infrared, the latter corrected for the contribution from the underlying white dwarf. Included in the figure is the spot model at orbital maximum, represented by a white dwarf model spectrum with $T_{\text{eff}} = 18500$ K.

The integrated flux in the thermal plasma X-ray component is $F_X = 6 \times 10^{-14}$ erg cm $^{-2}$ s $^{-1}$. At an assumed field strength of 13 MG (Beuermann et al. 2007) the cyclotron fundamental is at about $8 \mu\text{m}$. If we assume a Rayleigh-Jeans limited flux up to the H -band, where the cyclotron component peaks (Harrison et al. 2004 and Figs. 3 and 4), the integrated cyclotron flux is about $F_{\text{cyc}} \simeq 4 \times 10^{-12}$ erg cm $^{-2}$ s $^{-1}$. This value has an uncer-

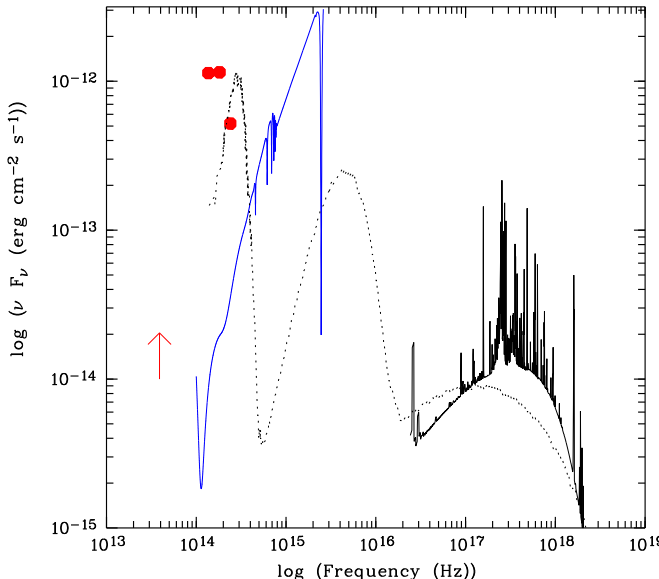


Fig. 4. Infrared to X-ray spectral energy distribution of EF Eri in the low state. Shown are radiation components which are associated with the accretion process, i.e. corrected for stellar photospheric radiation, at orbital maximum. The red arrow indicates the cyclotron fundamental for $B = 14$ MG.

tainty of at least 50%, since the cyclotron spectrum is covered only partly by observations.

There is no evidence for any component of re-processed radiation in the extreme ultraviolet/soft X-ray regime. We assume that the spot component in the ultraviolet carries the complete information on re-processed radiation. The integrated flux in this component is of order $F_{\text{rep}} \simeq 2 \times 10^{-11} \text{ erg cm}^{-2} \text{ s}^{-1}$. This is clearly larger than the primary cyclotron radiation and a factor ~ 300 larger than the thermal X-ray component. The large amount of radiation in the ultraviolet in excess of the primary radiation components is suggestive of a reservoir of heat from the previous high state and does not support a picture of instantaneous reprocessing. Clearly, more UV-observations are necessary to verify this picture by determining the cooling curve of the accretion spot.

We thus derive a flux balance $F_{\text{UV}} \simeq 5 \times F_{\text{cyc}}$ and $F_{\text{cyc}} \sim 60 F_X$, the latter ratio being suggestive of accretion in the bombardment regime at low mass flow rates and/or high magnetic field. The field of EF Eri is one of the lowest among all polars which made the binary a rather hard X-ray source with almost balanced flux contributions in the high state (see the detailed discussion in BSP87). Since Beuermann et al. found EF Eri to behave as described in the 'standard' accretion scenario (Lamb & Masters 1979), it was termed 'the textbook example of AM Herculis stars' by them. This picture changed fundamentally in the low state.

Beuermann (2004) presented a sequence of model spectra for $B = 14$ MG, $\Theta = 60^\circ$ and variable mass flow rate \dot{m} (in $\text{g cm}^{-2} \text{ s}^{-1}$). The values of B and Θ are quite similar to those of EF Eri. We include his model for $\dot{m} = 10^{-2} \text{ g cm}^{-2} \text{ s}^{-1}$ in Fig. 4. This model predicts the right (within an order of magnitude) flux ratio between cyclotron and X-ray flux. At

even lower mass flow rates, the next smaller value computed by Beuermann (2004) is $\dot{m} = 10^{-3} \text{ g cm}^{-2} \text{ s}^{-1}$, the flux ratio F_{cyc}/F_X becomes much smaller than observed. Also, the predicted size of the cyclotron emitting area would be larger than the white dwarf (for an assumed distance of 120 pc). We thus regard $\dot{m} = 10^{-2} \text{ g cm}^{-2} \text{ s}^{-1}$ as the likely value for EF Eri in its low accretion state. Fig. 4 shows the blackbody approximation as non-appropriate for the reprocessed component. This was noted already by Beuermann (2004), the low state observations of EF Eri prove this observationally.

At $\dot{m} = 10^{-2} \text{ g cm}^{-2} \text{ s}^{-1}$ and $B = 13$ MG the maximum predicted electron temperature is about 7 keV (Fischer & Beuermann 2001). Our measured temperature $kT \simeq 1.7$ keV (E501) indicates that the bulk of X-ray emission originates from denser layers at lower temperatures, as expected.

A comparison between high and low states fluxes of the main radiation components is instructive. For the mean fluxes in the high state, BSP87 derive $F_{\text{cyc}} = 4.8 \times 10^{-11} \text{ erg cm}^{-2} \text{ s}^{-1}$, $F_{\text{brems}} = 1.5 \times 10^{-10} \text{ erg cm}^{-2} \text{ s}^{-1}$, and $F_{\text{bb}} = 5.5 \times 10^{-10} \text{ erg cm}^{-2} \text{ s}^{-1}$, respectively. Hence, when switching from the high to the low state, the cyclotron flux is reduced by a factor ~ 10 , and the flux in the thermal plasma component by a factor 2500. These numbers illustrate the variable occupation of the different channels of energy release, when switching from a high-accretion rate, shock-dominated flow to the low-rate, cyclotron-dominated bombarded atmosphere. A direct comparison between the high- and low-state fluxes in the re-processed component seems not to be possible, since a counterpart to the high-state blackbody is missing in the low state. The low-state ultraviolet flux seems still to be fed high-state accretion heating.

The bolometric flux in the low state is $F_{\text{acc}} \simeq F_{\text{cyc}} \simeq 4 \times 10^{-12} \text{ erg cm}^{-2} \text{ s}^{-1}$, the luminosity is $L_{\text{acc}} \simeq 2\pi d^2 F_{\text{acc}} \simeq 2.4 \times 10^{30} d_{100}^2 \text{ erg s}^{-1}$, a factor 100 – 300 lower than the high state accretion luminosity derived by BSP87.

We may also compare the cyclotron emitting areas in the high and low states. BSP87 derive $A_{\text{cyc}} = (3.2 - 12.2) \times 10^{15} d_{100}^2 \text{ cm}^2$ while scaling of the model shown in Fig. 4 implies $A_{\text{cyc}} \simeq 30 \times 10^{15} d_{100}^2 \text{ cm}^2$. Again, care has to be taken by taking the latter number too literally since we have just scaled a pre-existing model, but they imply that the cyclotron emitting area has not shrunk by orders of magnitude.

A final comment may be made on EF Eri as a polar and its relation to the class of (likely misleadingly termed) LARPs (Low-Accretion Rate Polars; Schwone et al. 2002). The latter are close white dwarf/M dwarf pairs with pronounced cyclotron harmonics which led to their discovery in the HQS and the SDSS spectroscopic surveys. They are likely detached binaries accreting from the stellar wind of the secondary (Schmidt et al. 2005, Vogel et al. 2007). EF Eri is in a deep low state now for about 10 years. It is faint, its optical spectrum shows just the white dwarf and no secondary, variability in the optical is small, $\Delta V < 0.3^m$, its X-ray flux is faint and below all flux limits of surveys with sufficiently large survey area. Hence, all the classical discovery channels of CVs would not have led to the identification of EF Eri as a rather nearby cataclysmic variable in its extended low state. It would have been classified just as an isolated magnetic white dwarf in a spectroscopic survey.

But it shows an infrared excess, which could be (erroneously) interpreted as originating from a secondary and therefore would hint to the binary nature of this source. Actually it still shows a high degree of variability, although most pronounced in the ultraviolet. And finally, it still emits X-rays, but at the given flux the X-ray sky is dominated by AGNs. Hence, it still shows many hallmarks of the polars, and in that respect we may coin EF Eri as the textbook example of the low-accretion rate polars. We are not going to speculate about a population of missing CVs in similar extended low states. But the case of EF Eri as a secure low-accretion rate polar underlines the importance of a multi-wavelength approach to find more of these intriguing sources.

Acknowledgements. We thank our referee, Klaus Beuermann, for helpful comments which improved the manuscript. We thank V. Hambaryan and G. Lamer for help with the data reduction. This work was supported in part by the Deutsches Zentrum für Luft- und Raumfahrt (DLR) GmbH under contract No. FKZ 50 OR 0404 and by the Deutsche Forschungsgemeinschaft DFG under contract No. Schw536/20-1.

References

Bailey, J., Hough, J.H., Axon, D.J., et al., 1982, MNRAS 199, 801
 Beuermann, K., 2004, ASPC 315, 142
 Beuermann, K., Stella L., Patterson J., 1987, ApJ 316, 360 (BSP87)
 Beuermann, K., Wheatley, P., Ramsay, G., Euchner, F., Gänsicke, B.T., 2000, A&A 354, L49
 Beuermann, K., Euchner, F., Reinsch, K., Jordan, S., Gänsicke, B.T., 2007, A&A 463, 647
 Cropper, M., 1985, MNRAS 212, 709
 Harrison, T.E., Howell, S.B., Szkody, P., Homeier, D., Johnson, J.J., Osborne, H., 2004, ApJ 614, 947
 Koester, D., Napiwotzki, R., Voss, B., Homeier, D., Reimers, D., 2005, AA, 439, 317
 Meggitt, S.M.A., Wickramasinghe, D.T., 1989, MNRAS, 236, 31
 Nauenberg, M., 1972, ApJ 175, 417
 Piirola, V., Reiz, A., Coyne, G.V., S.J., 1987, A&A 186, 120
 Schmidt, G.D., Szkody, P., Vanlandingham, K.M., et al., 2005, ApJ 630, 1037
 Schwope, A., Brunner, H., Hambaryan, V., Schwarz, R., Staude, A., Szokoly, G., Hagen, H.-J., 2002, ASPC 261, 102
 Stelzer, B., Micela, G., Flaccomio, E., Neuhäuser, R., Jayawardhana, R., 2006, A&A 448, 293
 Szkody, P., Harrison, T.E., Plotkin, R.M., Howell, S.B., Seibert, M., Bianchi, L., 2006, ApJ 646, L147
 Thorstensen, J.R., 2003, AJ 126, 3017
 Vogel, J., Schwope, A.D., Gänsicke, B.T., 2007, A&A 464, 647
 Watson, M.G., King, A.R., Jones, M.H., Motch, C., 1989, MNRAS 237, 299
 Wheatley, P.J., Ramsay, G., 1998, ASPC 137, 446